Quantum computing of the ^{6}Li nucleus via ordered unitary coupled cluster

Oriel Kiss,[1,2,*] Michele Grossi,[1] Pavel Lougovski,[3]
Federico Sanchez,[4] Sofia Vallecorsa,[1] and Thomas Papenbrock[5,6]

[1] *European Organization for Nuclear Research (CERN), Geneva 1211, Switzerland*
[2] *Department of Computer Science, University of Geneva, Geneva 1211, Switzerland*
[3] *AWS Center for Quantum Computing, Seattle, Washington 98121, USA*
[4] *Department of Particle Physics, University of Geneva, Geneva 1211, Switzerland*
[5] *Department of Physics and Astronomy, University of Tennessee, Knoxville, Tennessee 37996, USA*
[6] *Physics Division, Oak Ridge National Laboratory, Oak Ridge, Tennessee 37831, USA*

(Dated: May 3, 2022)

The variational quantum eigensolver (VQE) is an algorithm to compute ground and excited state energy of quantum many-body systems. A key component of the algorithm and an active research area is the construction of a parametrized trial wavefunction – a so called variational ansatz. The wavefunction parametrization should be expressive enough, i.e. represent the true eigenstate of a quantum system for some choice of parameter values. On the other hand, it should be trainable, i.e. the number of parameters should not grow exponentially with the size of the system. Here, we apply VQE to the problem of finding ground and excited state energies of the odd-odd nucleus ^{6}Li. We study the effects of ordering fermionic excitation operators in the unitary coupled clusters ansatz on the VQE algorithm convergence by using only operators preserving the J_z quantum number. The accuracy is improved by two order of magnitude in the case of descending order. We first compute optimal ansatz parameter values using a classical state-vector simulator with arbitrary measurement accuracy and then use those values to evaluate energy eigenstates of ^{6}Li on a superconducting quantum chip from IBM. We post-process the results by using error mitigation techniques and are able to reproduce the exact energy with an error of 3.8% and 0.1% for the ground state and for the first excited state of ^{6}Li, respectively.

I. INTRODUCTION

The simulation of static and dynamic properties of quantum many-body systems is a challenging task for classical computers due to the exponential scaling of the Hilbert space. In contrast, quantum computers could be natural devices to solve such problems [1], avoiding the exponential scaling. For example, quantum algorithms such as the quantum phase estimation (QPE) [2] and imaginary time evolution [3], can perform eigenvalues calculations in polynomial time [4] using future quantum error-corrected hardware. Currently, the circuit depth required to implement them is far greater than that of state-of-the-art noisy intermediates scale quantum (NISQ) [5] devices. Nevertheless, NISQ devices have attracted a lot of interest in nuclear physics [6–19]. Presently available quantum hardware can be used to compute the ground-state energy E_0 of a Hamiltonian H by using the variational principle. The variational quantum eigensolver (VQE) [20–22] is a hybrid quantum-classical algorithm [23] which classically minimizes the expectation value of a trial wavefunction in the form of a parametrized quantum circuit [24]

$$E_0 \leq \frac{\langle\psi(\theta)|\, H\, |\psi(\theta)\rangle}{\langle\psi(\theta)|\psi(\theta)\rangle}. \tag{1}$$

The trainability of the VQE is closely related to the chosen wavefunction ansatz. It has to be expressive enough to contain the optimal solutions yet simple enough to enable training and to avoid unpleasant effects like the barren plateaus [25]. Hardware efficient [26] and physically inspired ansätze [27] are popular choices for this task. The former is as shallow as possible in the circuit architecture, with the smallest number of CNOT gates executable on NISQ devices, whereas the latter is built according to properties of the underlying physical system. Although VQE simulations have been widely and successfully used in quantum chemistry [20, 21, 26–30], there are fewer applications in nuclear physics [6, 12, 14–16]. While both fields share many similarities, such as being formulated as non-relativistic quantum field theories in second quantization, they differ in many other aspects. For instance, protons and neutrons, the equivalent of α and β electrons in quantum chemistry, interact via strong and short-ranged forces, and symmetry breaking, i.e. nuclear deformation and superfluidity, is abundant. This makes it important to reflect this physics in the quantum circuit [14].

Starting from the work [14] on atomic nuclei, we study several training strategies for the convergence of different ansätze for the ^{6}Li nucleus and evaluate our results on superconducting quantum hardware. We note that the papers [14, 16] focused on even-even nuclei, which are simpler in structure than the odd-odd nucleus ^{6}Li. This makes the problem an interesting step toward VQE applications in nuclear physics.

* oriel.kiss@cern.ch

This paper is organized as follows. We define the theoretical framework in Sec. II, introduce the model in Sec. II A, and present the different ansätze used in the present work in Sec. II C. We present results for the energies of the ground-state and first excited states obtained from simulations in Sec. III B and from superconducting quantum hardware in Sec. III C.

II. THEORETICAL FRAMEWORK

We consider a simple shell model where the nucleus ^{6}Li is described as a valence proton and neutron added to the inert ^{4}He core. In this Section, we describe the model space and Hamiltonian, present the unitary coupled-cluster ansatz, and discuss in detail the ordering and implementation of the excitation operators.

A. Model space

The model space consists of the $0p_{3/2}$ and $0p_{1/2}$ harmonic oscillator orbitals for the neutron and the proton, and we use the Cohen-Kurath interaction [31]. Our work builds on the recent computation of ^{6}He in the same framework [14] and extends it to a somewhat larger Hilbert space and a somewhat more complicated nucleus. In addition to being realistic and non-trivial, our model has the advantage of being simple enough to be run on current NISQ devices. The Hamiltonian can be written in second quantization as

$$H = \sum_i \epsilon_i \hat{a}_i^\dagger \hat{a}_i + \frac{1}{2}\sum_{ijkl} V_{ijlk} \hat{a}_i^\dagger \hat{a}_j^\dagger \hat{a}_k \hat{a}_l \ . \tag{2}$$

Here, $\hat{a}_i^\dagger$ and $\hat{a}_i$ are the creation and annihilation operators , respectively, for a nucleon in the state $|i\rangle$. The single-particle energies are denoted as ϵ_i and two-body matrix elements as V_{ijkl}. All computed energies are with respect to the ground-state energy of the ^{4}He core.

We have $|i\rangle = |n = 0, l = 1, j, j_z, t_z\rangle$ where n and l denote the radial and orbital angular momentum quantum numbers, respectively, $j = 1/2, 3/2$ the total spin, j_z its projection, and $t_z = \pm 1/2$ the isospin projection. Thus, the p shell model space includes six orbitals for the protons and six orbitals for the neutrons, and we need $N = 12$ qubits, one per orbital. The Cohen-Kurath interaction preserves total spin J and total isospin T, and their projections J_z and T_z. We will exploit that J_z and T_z are conserved in our wavefunction ansatz.

We convert the shell-model Hamiltonian (2) into a qubit Hamiltonian via the Jordan-Wigner [32] transformation, i.e. we have the mapping

$$\hat{a}_i^\dagger = \frac{1}{2}\left(\prod_{j=0}^{i-1} -Z_j\right)(X_i - iY_i), \tag{3}$$

qubit	j	j_z	t_z
0	1/2	−1/2	−1/2
1	1/2	+1/2	−1/2
2	3/2	−3/2	−1/2
3	3/2	−1/2	−1/2
4	3/2	+1/2	−1/2
5	3/2	+3/2	−1/2
6	1/2	−1/2	+1/2
7	1/2	+1/2	+1/2
8	3/2	−3/2	+1/2
9	3/2	−1/2	+1/2
10	3/2	+1/2	+1/2
11	3/2	+3/2	+1/2

Table I. Orbitals represented by the different qubits. Here, j is the total angular momentum, j_z its projection on the z axis and t_z is the third component of the isospin.

$$\hat{a}_i = \frac{1}{2}\left(\prod_{j=0}^{i-1} -Z_j\right)(X_i + iY_i), \tag{4}$$

where X_i, Y_i and Z_i are the Pauli matrices acting on the i^{th} qubit. The Bravyi-Kitaev [33] mapping is an alternative to Jordan-Wigner that achieves exponentially shorter Pauli strings in the asymptotic limit. However, both transformations perform similarly for modest systems sizes [34]. As only the Jordan-Wigner mapping enjoys an intuitive translation of the J_z symmetry on the qubit system we will only consider this mapping here. Each single-particle state is represented by a qubit where $|0\rangle$ and $|1\rangle$ refer to an empty and an occupied state, respectively. For completeness, we list the different states in Table I.

Despite the simplicity of our model, the Hamiltonian (2) consists of 975 Pauli terms. This large number arises because the short-range nuclear interaction is nonlocal when expressed in the harmonic-oscillator basis, and the number of Pauli terms naively scales as n^4, which is reduced by an order of magnitude because of the conservation of spin and isospin. Eventually, it could be an advantage to use a lattice formulation [35] where the short range of the nuclear interaction reduces the number of Pauli terms. At this moment, however, the minimum $2 \times 2 \times 2$ lattice requires 32 qubits because of spin and isospin degrees of freedom, and our smaller shell-model space yields more realistic results.

We deal with the large number of Pauli terms by grouping them into 250 sets of qubit-wise commuting operators. Commuting operators are simultaneously diagonalizable, allowing the computation of the expectation value from the measurements of a single circuit. Additional techniques exist to reduce further the number

of circuits. References [36, 37] propose to further group the Pauli operators to include general commutating operators at the cost of appending a circuit with $\mathcal{O}(N^2)$ gates before the measurements. General commutating operators $\mathcal{O}^1, \mathcal{O}^2$ satisfy $[\mathcal{O}^1, \mathcal{O}^2] = 0$ whereas qubit-wise commuting operators $[\mathcal{O}_i^1, \mathcal{O}_i^2] = 0$ for all i. Ref. [38] obtained a cubic reduction by using low-rank factorization. It is even possible to reduce the measurements to a single operator [39], by using quantum information complete measurements at the cost of a higher number of shots and ancillas. Nonetheless, currently available resources for this work were enough to evaluate the whole Hamiltonian with the qubit-wise commutating grouping. We consequently followed this technique to avoid deeper circuits.

B. The unitary coupled cluster ansatz

The *unitary coupled clusters ansatz (UCC)* is widely used to obtain a correlated ground-state from an initial Hartree-Fock solution $|\psi_0\rangle$ in quantum chemistry and nuclear physics [28, 29, 40]. It lets the Hartree-Fock state evolve according to the cluster operator $\hat{T}$. To be compatible with a quantum computing paradigm, the operator has to be unitary. Therefore we choose

$$|\psi(\boldsymbol{\theta})\rangle = e^{i\left(\hat{T}(\boldsymbol{\theta}) - \hat{T}^\dagger(\boldsymbol{\theta})\right)} |\psi_0\rangle \,. \tag{5}$$

$\hat{T}$ can be decomposed into singles, i.e. 1-particle–1-hole (1p-1h), doubles (2p-2h), ..., excitation operators of the following form

$$\hat{T} = \hat{T}_1 + \hat{T}_2 + \dots \tag{6}$$

with

$$\hat{T}_1 = \sum_{i \in \text{virt}; \alpha \in \text{occ}} \theta_i^\alpha \hat{a}_i^\dagger \hat{a}_\alpha \tag{7}$$

and

$$\hat{T}_2 = \sum_{i,j \in \text{virt}; \alpha,\beta \in \text{occ}} \theta_{ij}^{\alpha\beta} \hat{a}_i^\dagger \hat{a}_j^\dagger \hat{a}_\alpha \hat{a}_\beta . \tag{8}$$

In the above definitions, the Latin indices run over virtual (empty) states and the Greek over occupied states of the initial state. The cluster operator drives occupied orbitals to empty ones. To respect symmetries and reduce the number of terms, we only considered excitations with a total angular-momentum projection $J_z = 0$. The Jordan-Wigner mapping is then used to transform the unitary cluster ansatz into a qubit operator with trainable parameters $\boldsymbol{\theta}$. The UCC ansatz is finally constructed with the time evolution of these excitation operators, which is implemented using Trotterization with one step.

The *Initial State* $|\psi_0\rangle$ is usually chosen as the Hartree-Fock solution. However, it is often sufficient to lie close enough to the actual ground-state. For instance, the ^{6}Li ground-state has spin $J = 1$ and therefore $J_z = -1, 0$ or 1. So, any product state with this configuration, e.g. $|1\rangle \otimes |6\rangle$ or $|0\rangle \otimes |7\rangle$ should converge to the ground-state. Moreover, this observation can help us find the first excited state (with spin $J = 3$), which lies in the subspace with a total J_z of -3, -2, 2, or 3 orthogonal to the ground state. This observation provides a particular advantage over other methods in finding excited states with the VQE, such as the iterative constrained optimization [41], the discriminative VQE [42], or those based on the quantum equation of motion [43]. These techniques require additional quantum or classical resources and rely on the accuracy of the prepared ground-state, therefore suffering from the error amplification phenomenon. On the other hand, enforcing the ansatz to stay in a particular region of the Hilbert space by choosing the right quantum numbers, produces stable and accurate solutions which are easy to obtain when applicable.

C. Excitation ordering

In the following, we describe different strategies to study the convergence of the variational method. The ordering of the excitation operators impacts the training landscape and the convergence behavior. Hence, an ansatz may quickly converge while another remains trapped in a local minimum. We observed this in our work by trying different ordering.

Shuffling is a strategy that consists of choosing the best sorting over multiple runs with a random shuffling, and it yields good convergence. However, it quickly becomes prohibitive to explore the shuffled space when enlarging the system size. Nevertheless, the ordering has a non-trivial effect on the optimization procedure. We will refer to this strategy as *best shuffle* throughout this paper.

Ordering represents a second option, where we proceed to order the operators by their absolute magnitude of the corresponding term in the Hamiltonian. Hence, the singles excitation refers to the corresponding single-particle energy ϵ_i while the doubles excitation $\hat{a}_i^\dagger \hat{a}_j^\dagger \hat{a}_\alpha \hat{a}_\beta$ refers to the two-body term $V_{ij\beta\alpha}$. The considered Hamiltonian permits only to apply this ordering on singles and doubles terms, but more complex models could be considered to order 3p-3h or 4p-4h excitation as well. This approach, similar to the QDrift [44] algorithm for time evolution (which chooses the terms randomly to be evolved according to their relative magnitude), orders the excitation operator in descending order of magnitude such that the most important ones are placed at the beginning. We observed that this technique, which we will refer to as *ordered* UCCSD, is the most promising ansatz among the ones considered in this work. Moreover, when coupled to a layerwise learning

scheme, it achieves arbitrary accuracy in a polynomial number of optimization steps.

Adaptive Derivative-Assembled Problem-Tailored (ADAPT)-VQE is another efficient strategy to adaptively order the operators with respect to the magnitude of their gradient. ADAPT-VQE [30] constructs the ansatz by picking from a pool of operators $\{\hat{\tau}_0, \ldots, \hat{\tau}_n\}$ the one which has the most impact on the expectation value, namely the one with the largest gradient magnitude

$$\left|\frac{\partial E}{\partial \theta_i}\right|_{\theta_i=0} = |\langle\psi|[H, \hat{\tau}_i]|\psi\rangle|. \tag{9}$$

The chosen operator is recursively added to the current ansatz, leading to

$$|\psi(\boldsymbol{\theta})\rangle = e^{-i\theta_l \tau_l} e^{-i\theta_{l-1}\tau_{l-1}} \ldots e^{-i\theta_0\tau_0} |\psi_0\rangle, \tag{10}$$

after adding l operators. We set $\theta_l = 0$ to allow a smooth transition between the architecture's update. The picking action is followed by k optimization steps, and it is repeated until convergence is reached. It generally leads to accurate solutions with minimal depth. The computation of the gradients of all the operators in the pool, which is time-consuming, can in principle be performed in parallel. We note that Ref. [30] uses $k = 1$. However, we found useful to choose $k = 10$. This permits to perform more optimization steps while keeping the ansatz shallow.

Grimsley *et al.* [30] demonstrated with numerical experiments that ADAPT-VQE is superior to random or lexical ordering of the excitation operators in terms of convergence and circuit depth. However, our study suggests that reducing the operator pool using symmetries and ordering with respect to their magnitude achieves quicker convergence. Studies of the Lipkin-Meshkov-Glick model [16] showed that the number of operators needed to achieve 1% accuracy increases linearly with the number of valence neutrons. However, this behavior has only been simulated within nuclei with an even number of valence neutrons and without valence protons: it remains an open question whether this result also holds with neutron-proton interactions.

Finally, we consider *layerwise learning*, a technique initially proposed to mitigate barren plateaus in quantum machine learning [45]. The idea is to consider m singles terms first, perform k optimization steps, add m new singles terms, and continue until all singles terms have been used before moving to higher-order interactions. In an ordered approach, the first k operators added to the ansatz are instead chosen according to the selected ordering.

D. Hardware efficient ansatz

Because of the Jordan Wigner mapping, fermionic excitation operators act on $\mathcal{O}(N)$ qubits. Therefore, they are expensive for NISQ devices due to the increased connectivity required and the consequent increase in the number of CNOT and Swap gates needed after circuit transpilation. A simple and alternative way to reduce this expense is to consider qubit-based excitation (QBE) [46, 47] operators. QBE efficiently implements the excitation operators on $\mathcal{O}(1)$ qubits by neglecting the Z terms in the Jordan Wigner mapping. Essentially, creation operators are mapped to

$$\hat{a}_i^\dagger = \frac{1}{2}(X_i - iY_i), \tag{11}$$

and annihilation operators to

$$\hat{a}_i = \frac{1}{2}(X_i + iY_i). \tag{12}$$

The difference between a Jordan Wigner mapping is that the resulting operator will not respect fermionic anti-commutation relations, which are enforced by the product of Pauli Z matrices. Single excitation operators between qubits i and j read

$$U_{ij}(\theta) = \exp\left[i\frac{\theta}{2}(X_iY_j - Y_iX_j)\right] \tag{13}$$

and double excitation operator between qubits i, j, k and l are

$$\begin{aligned} U_{ijkl}(\theta) = \exp\Big[i\frac{\theta}{8}(&X_iY_jX_kX_l + Y_iX_jX_kX_l \\ &+Y_iY_jY_kX_l + Y_iY_jX_kY_l \\ &-X_iX_jY_kX_l - X_iX_jX_kY_l \\ &-Y_iX_jY_kY_l - X_iY_jY_kY_l)\Big]. \end{aligned} \tag{14}$$

Even if QBE-UCC ansätze do not respect the fermionic anti-commutation relations, they show a comparable efficiency for ground-state calculations. Those ansätze are hardware efficient as they act on a fixed number of qubits (2 for the singles, 4 for the doubles, and 2^k for the k-th excitation operators). The exact circuit formulation can be found in the original paper [46].

Finally, we also considered an efficient excitation-preserving ansatz, such as the one proposed in [26] for quantum chemistry. These ansätze are constructed with gates preserving the number of occupied orbitals. Moreover, time-reversal symmetry can lead to further simplifications. They have the advantage of using fewer CNOT gates resulting in a more shallow circuit, an advantage for near-time devices. However, they cannot respect the total J_z symmetry as they act on the protons and neutrons separately. In our investigations, this led to circuits suffering from barren plateaus [25] which are expected in

generic circuits using a global cost function [48], such as the expectation value of the Hamiltonian. We remark that the gradient vanishes from the beginning, and changing the number of layers, optimizer, learning rate, parameters initialization, and even using an automatic differentiation framework to compute the gradient did not permit us to train the ansatz. This observation suggests that symmetries play a non-negligible role in nuclear structure calculations since it is the significant difference between UCC based ansätze and excitation preserving ones.

III. RESULTS

In the following, we present the results obtained with the different circuit architectures discussed in Sec. II C. The investigations were performed on a statevector simulator and the hardware-friendly QBE-UCCSD ansatz was evaluated on a real quantum processor.

Statevector simulations allow one to probe the potential of this approach under ideal conditions, such as using exponentially many shots or without noise. UCC ansätze are notoriously deep, and the noise heavily deteriorates the outcome, even when using error mitigation techniques. We address these difficulties in the following, showing the results step by step.

A. Optimization

For the optimization we use the simultaneous perturbation stochastic approximation (SPSA) [49] with a fixed number of iterations. SPSA efficiently approximates the gradient with two circuit evaluations by shifting the parameters in two random directions. The learning rate $\texttt{lr} = 0.1$, is halved at every 25 iterations until $\texttt{lr} = 0.001$ to ensure a fast convergence at the beginning and to avoid oscillations at the end. Looking at realistic experiments, the stochastic nature of SPSA makes it resilient to the statistical noise coming from the finite number of measurements, making it appealing for quantum devices. All the initial parameters, except the first one, are set to zero at the beginning of the optimization in an attempt to mitigate barren plateaus [50], while the first is chosen at random between 0 and 2π, but fixed across the different ansätze. We remark that the value of the first parameter has a negligible effect on the convergence.

A variant of the SPSA optimizer using the geometry of the Hilbert space has been recently proposed [51]. It uses six circuit evaluations to approximate the Hessian (which can be used to compute the quantum natural gradient) and significantly improves the optimization efficiency of quantum circuits. In the present work, the effect of the quantum natural gradient was mainly appreciated on hardware-friendly ansatz such as the QBE-UCC.

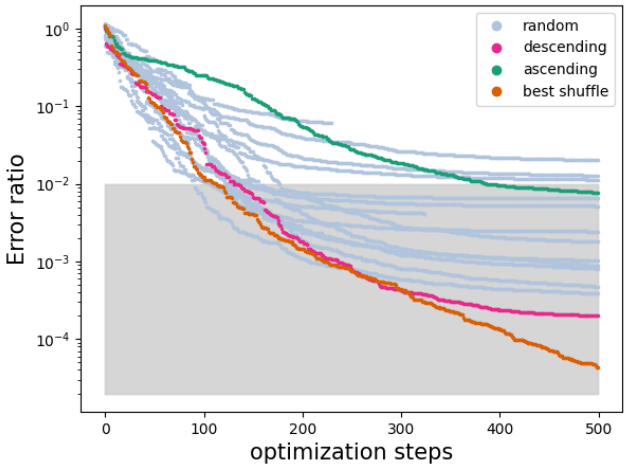

Figure 1. Training curve in a semilog scale for fermionic UCC ansatz with different ordering. The *best shuffle* curve is taken among 20 independent runs. The grey area corresponds to the 1% margin, which is acceptable in most applications.

B. State-vector simulations

The gate-based quantum circuits used in this section were built using the open-source framework `qiskit-nature` [52] and were run on pennylane [53] using the C++ `lightning.qubit` plugin.

We first assess the effect of *ordering* on the fermionic-UCC ansatz starting from the initial state $|2\rangle\otimes|11\rangle$. This state has $J_z = 0$, and has the largest operator pool on which we perform 500 optimization steps. The optimization curve, which shows the error ratio

$$\text{error ratio} = \left|\frac{E_{\text{VQE}} - E_{\text{exact}}}{E_{\text{exact}}}\right|, \tag{15}$$

for different ordering is shown in Fig. 1. We observe that the descending ordering (pink) strategy leads to fast convergence while the ascending ordering (green) strategy converges slowly. Thus, most important operators should be placed first. We also note that a favorable convergence trend is also given by the *best shuffle* curve (orange), which is taken among 20 independent runs, and by some random run combinations, for which the relative differences are not easily interpreted.

a. Ground state calculation We now compare the different ansätze presented in Sec. II C to prepare the ground state. For the fermionic-UCC ansatz, we start again from $|2\rangle \otimes |11\rangle$ state, and we train with the SPSA optimizer. In the iterative approach (ADAPT-VQE, Layerwise Learning), $k = 10$ iterations are performed between each architecture update. This choice has shown to be a good trade-off between a slow convergence (for large k) and deep circuits (for small k). For the

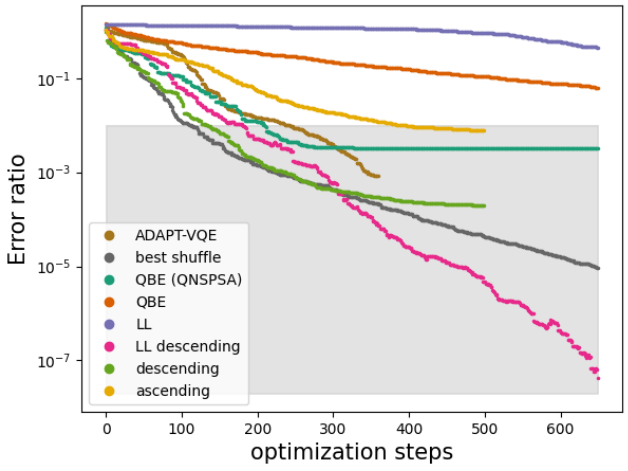

Figure 2. Training curve in a semilog scale for all different ansätze with different training strategies. The grey area corresponds to the 1% margin, which is acceptable in most applications.

QBE-UCC ansatz, it has been experienced that it is preferable to start from the state $|0\rangle \otimes |7\rangle$, which also has the smallest operator pools and is consequently better suited for noisy devices.

The learning curves are shown in Fig. 2 and we observe that descending ordering strategies are among the fastest and more accurate ones, the best being the layerwise learning with descending ordering (pink). Interestingly, the ADAPT-VQE (brown) approach does not perform as well as the former. We suspect that the gradient evaluated at $\theta = 0$ does not contain enough information to obtain the optimal solution. On the one hand, the circuit at the beginning contains not enough operators, which explains the slow convergence curve. On the other hand, the algorithm mainly picks the same operators which may prevent convergence to the optimal solution. Hence, it only used half of the available operators before becoming too deep to be trained efficiently.

The quantum natural SPSA optimizer significantly improves the optimization of the QBE-UCC ansatz, compared to the standard SPSA. This can be seen by comparing the QBE (QNSPSA) curve (dark green) with the QBE (orange) one. The descending ordered UCC ansatz achieves an exponentially fast convergence, and the descending layerwise learning strategy reaches arbitrary accuracy.

b. First excited state As pointed out in Sec. II B, the choice of the initial state allows us to find the first excited state easily. Hence, an initial state with $J_z = -3, -2, 2$ or 3 will remain in a subspace is orthogonal to the ground state. For instance, the state $|1\rangle \otimes |11\rangle$ has $J_z = 2$ and it is therefore a possible candidate. The result obtained in this case, for a fermionic UCC ansatz optimized on a statevector simulator, achieves an error ratio of 10^{-11}.

C. Hardware

We evaluate the most hardware-efficient ansatz, i.e. QBE-UCC, previously trained on the statevector simulator, on a superconducting chip from IBM. Gate-based quantum circuits, ran on the cloud using the IBM Quantum Lab, were transpiled onto the hardware topology by using the SWAP-based BidiRectional (SABRE) heuristic search algorithm [54]. Multiple runs were performed to select the circuit which minimized the total number of CNOT gates needed. The SABRE algorithm enabled a 50% CNOT reduction compared to a naive approach for a total of 209 CNOTs. Measurement error mitigation was performed efficiently, as proposed in Ref. [55], by individually inverting the error matrices

$$S_k = \begin{pmatrix} P^{(k)}_{0,0} & P^{(k)}_{0,1} \\ P^{(k)}_{1,0} & P^{(k)}_{1,1} \end{pmatrix}. \tag{16}$$

Here, $P^{(k)}_{i,j}$ is the probability of the k-th qubit to be in state $j \in \{0, 1\}$ while measured in state $i \in \{0, 1\}$. While this only corrects the uncorrelated readout errors, it is argued in Ref. [55] that they are the predominant ones, making it a useful tool for measurement error mitigation for large number of qubits.

Regarding CNOT errors, the zero-noise extrapolation [56–58] represents a powerful mitigation technique by artificially stretching the noise to be extrapolated to the noise-less regime. However, the structure of the considered Hamiltonian amplified the effect of CNOT errors considerably and prevented us from using this strategy. Hence, states with a wrong number of occupied orbitals belong to different nuclei, which can have much lower energy. We observed a discrepancy of almost 300% by stretching the noise with a factor two and did not investigate zero-noise extrapolation further.

Our tests were executed on the IBM Quantum 27 qubits architecture *ibmq_mumbai* and repeated 10 times for the ground-state and 5 for the first excited state, using 8092 shots each. The results are reported in Table II, alongside the number of parameters and CNOT gates after transpilation. We observe that the energy is reproduced up to 3.81% and 0.12% accuracy for the ground- and first excited state, respectively. Both lie within one standard deviation confidence interval. Moreover, the standard deviation for the ground-state is ten times smaller than the energy gap with the first excited state, which accentuates the accuracy of our results. We remark that measurement error mitigation increases the accuracy by more than 10%, making it appealing for readout error mitigation in quantum circuits with a large number of qubits.

hardware	# parameters	# CNOT	mean	st. deviation	exact	error ratio
ibmq_mumbai raw (gs)	9	209	-6.27	0.269	-5.529	13.36%
ibmq_mumbai mittigated (gs)	9	209	-5.319	0.24	-5.529	3.81%
ibmq_mumbai raw (1st es)	3	41	-2.907	0.87	-3.420	14.97%
ibmq_mumbai mittigated (1st es)	3	41	-3.424	0.08	-3.420	0.12%

Table II. Hardware results of the QBE-UCC ansats for the ground-state (gs) and first excited state (1st es), alongside the number of parameters and CNOT gates after transpilation. The exact result, obtained with exact diagonalization, are reproduced up to one standard deviation.

IV. CONCLUSIONS

We performed shell-model quantum-computations of the nucleus ^{6}Li, composed of a frozen ^{4}He core and two valence nucleons. We studied the effect of the ordering of excitation operators in unitary coupled clusters type ansätze for the variational quantum eigensolver. We empirically observed that the ordering strongly affects the learning curve and that arranging in descending order of magnitude with respect to the Hamiltonian leads to a better convergence behavior than random ordering or ADAPT-VQE. Hence, operators with high magnitude have more importance in the system's description, which should be reflected in the ansatz construction. Moreover, adopting a layerwise learning scheme, where the operators are iteratively added to the circuit, has shown an accuracy of the order of 10^{-7}. By choosing an initial state with a suitable J_z quantum number, we were also able to compute the energy of the first excited state with a precision of 10^{-11}.

Finally, we evaluated the qubit based excitation-UCC (QBE-UCC), which neglects the fermionic anti-commutation relation to reduce the number of CNOT and SWAP gates needed. We performed, for the first time to our knowledge, these calculations on a real quantum device, a 27 qubits machine (*ibmq_mumbai*), and we were able to reproduce the exact ground state and first excited state energy up to one standard deviation.

The number of nuclear states grows factorially with the number of valence nucleons, making the scaling of VQE applications impractical. Even if the numbers of singles and doubles excitation operators seem to grow linearly [16], it may be necessary to use triples and quadruples excitation operators as well. Reference [14] demonstrated that quadruple operators acting on all valence nucleons were necessary in a UCC ansatz for a ^{8}Be nucleus, composed of two protons and two neutrons in the p-shell, and achieved 1% error ratio on statevector simulations with 118 parameters. This motivates symmetry considerations to reduce the number of operators, in order to prevent deep ansätze, which are not easily trainable, while keeping all the operators needed to reproduce the exact energy. This will be the focus of future research in this direction.

ACKNOWLEDGMENTS

We thank Zhonghao Sun for helping with the nuclear matrix elements. This work was supported by CERN Quantum Technology Initiative, the U.S. Department of Energy, Office of Science, Office of Nuclear Physics, under Award Nos. DE-FG02-96ER40963 and DE-SC0021642, and by the Quantum Science Center, a National Quantum Information Science Research Center of the U.S. Department of Energy. Oak Ridge National Laboratory is supported by the Office of Science of the U.S. Department of Energy under contract No. DE-AC05-00OR22725. Access to the IBM Quantum Services was obtained through the IBM Quantum Hub at CERN. The views expressed are those of the authors and do not reflect the official policy or position of IBM, the IBM Q team or AWS.

[1] Richard P. Feynman, "Simulating physics with computers," International Journal of Theoretical Physics **21**, 467–488 (1982).
[2] A.Yu.Kitaev, "Quantum measurements and the abelian stabilizer problem," ArXiv e-prints (1995), arXiv:9511026 [quant-ph].
[3] Kübra Yeter-Aydeniz, Raphael C. Pooser, and George Siopsis, "Practical quantum computation of chemical and nuclear energy levels using quantum imaginary time evolution and lanczos algorithms," npj Quantum Inf **6**, 63 (2020).
[4] Daniel S. Abrams and Seth Lloyd, "Quantum algorithm providing exponential speed increase for finding eigenvalues and eigenvectors," Phys. Rev. Lett. **83**, 5162–5165 (1999).
[5] John Preskill, "Quantum Computing in the NISQ era and beyond," Quantum **2**, 79 (2018).
[6] E. F. Dumitrescu, A. J. McCaskey, G. Hagen, G. R. Jansen, T. D. Morris, T. Papenbrock, R. C. Pooser, D. J. Dean, and P. Lougovski, "Cloud quantum computing of

an atomic nucleus," Phys. Rev. Lett. **120**, 210501 (2018).
[7] N. Klco, E. F. Dumitrescu, A. J. McCaskey, T. D. Morris, R. C. Pooser, M. Sanz, E. Solano, P. Lougovski, and M. J. Savage, "Quantum-classical computation of schwinger model dynamics using quantum computers," Phys. Rev. A **98**, 032331 (2018).
[8] Hsuan-Hao Lu, Natalie Klco, Joseph M. Lukens, Titus D. Morris, Aaina Bansal, Andreas Ekström, Gaute Hagen, Thomas Papenbrock, Andrew M. Weiner, Martin J. Savage, and Pavel Lougovski, "Simulations of subatomic many-body physics on a quantum frequency processor," Phys. Rev. A **100**, 012320 (2019).
[9] Alessandro Roggero and Joseph Carlson, "Dynamic linear response quantum algorithm," Phys. Rev. C **100**, 034610 (2019).
[10] Alessandro Roggero, Andy C. Y. Li, Joseph Carlson, Rajan Gupta, and Gabriel N. Perdue, "Quantum computing for neutrino-nucleus scattering," Phys. Rev. D **101**, 074038 (2020).
[11] Alessandro Roggero, Chenyi Gu, Alessandro Baroni, and Thomas Papenbrock, "Preparation of excited states for nuclear dynamics on a quantum computer," Phys. Rev. C **102**, 064624 (2020).
[12] Michael J. Cervia, A. B. Balantekin, S. N. Coppersmith, Calvin W. Johnson, Peter J. Love, C. Poole, K. Robbins, and M. Saffman, "Lipkin model on a quantum computer," Phys. Rev. C **104**, 024305 (2021).
[13] Weijie Du, James P. Vary, Xingbo Zhao, and Wei Zuo, "Quantum simulation of nuclear inelastic scattering," Phys. Rev. A **104**, 012611 (2021).
[14] I. Stetcu, A. Baroni, and J. Carlson, "Variational approaches to constructing the many-body nuclear ground state for quantum computing," ArXiv e-prints (2021), arXiv:2110.06098 [nucl-th].
[15] Wenyang Qian, Robert Basili, Soham Pal, Glenn Luecke, and James P. Vary, "Solving hadron structures using the basis light-front quantization approach on quantum computers," (2021), arXiv:2112.01927 [quant-ph].
[16] A.M. Romero, J. Engel, Ho Lun Tang, and Sophia E. Economou, "Solving nuclear structure problems with the adaptive variational quantum algorithm," ArXiv e-prints (2022), arXiv:2203.01619 [nucl-th].
[17] A. Baroni, J. Carlson, R. Gupta, Andy C. Y. Li, G. N. Perdue, and A. Roggero, "Nuclear two point correlation functions on a quantum computer," Phys. Rev. D **105**, 074503 (2022).
[18] F. Turro, A. Roggero, V. Amitrano, P. Luchi, K. A. Wendt, J. L. Dubois, S. Quaglioni, and F. Pederiva, "Imaginary-time propagation on a quantum chip," Phys. Rev. A **105**, 022440 (2022).
[19] Manqoba Q. Hlatshwayo, Yinu Zhang, Herlik Wibowo, Ryan LaRose, Denis Lacroix, and Elena Litvinova, "Simulating excited states of the Lipkin model on a quantum computer," (2022), arXiv:2203.01478 [nucl-th].
[20] Alberto Peruzzo, Jarrod McClean, Peter Shadbolt, Man-Hong Yung, Xiao-Qi Zhou, Peter J. Love, Alán Aspuru-Guzik, and Jeremy L. O'Brien, "A variational eigenvalue solver on a photonic quantum processor," Nature Communications **5**, 4123 (2014).
[21] Abhinav Kandala, Antonio Mezzacapo, Kristan Temme, Maika Takita, Markus Brink, Jerry M. Chow, and Jay M. Gambetta, "Hardware-efficient variational quantum eigensolver for small molecules and quantum magnets," Nature **549**, 242–246 (2017).
[22] Dmitry A. Fedorov, Bo Peng, Niranjan Govind, and Yuri Alexeev, "Vqe method: a short survey and recent developments," Mater Theory **6**, 2 (2022).
[23] Jarrod R McClean, Jonathan Romero, Ryan Babbush, and Alán Aspuru-Guzik, "The theory of variational hybrid quantum-classical algorithms," New Journal of Physics **18**, 023023 (2016).
[24] Marcello Benedetti1, Erika Lloyd, Stefan Sack, and Mattia Fiorentini, "Parameterized quantum circuits as machine learning models," Quantum Science and Technology **4**, 4 (2019).
[25] Jarrod R. McClean, Sergio Boixo, Vadim N. Smelyanskiy, Ryan Babbush, and Hartmut Neven, "Barren plateaus in quantum neural network training landscapes," Nature Communications **9**, 4812 (2018).
[26] Panagiotis Kl. Barkoutsos, Jerome F. Gonthier, Igor Sokolov, Nikolaj Moll, Gian Salis, Andreas Fuhrer, Marc Ganzhorn, Daniel J. Egger, Matthias Troyer, Antonio Mezzacapo, Stefan Filipp, and Ivano Tavernelli, "Quantum algorithms for electronic structure calculations: Particle-hole hamiltonian and optimized wavefunction expansions," Phys. Rev. A **98**, 022322 (2018).
[27] Luca Crippa, Francesco Tacchino, Mario Chizzini, Antonello Aita, Michele Grossi, Alessandro Chiesa, Paolo Santini, Ivano Tavernelli, and Stefano Carretta, "Simulating static and dynamic properties of magnetic molecules with prototype quantum computers," Magnetochemistry **7** (2021), 10.3390/magnetochemistry7080117.
[28] Qing Guo and Ping-Xing Chen, "Optimization of vqe-ucc algorithm based on spin state symmetry," Frontiers in Physics **9** (2021), 10.3389/fphy.2021.735321.
[29] Jonathan Romero, Ryan Babbush, Jarrod R McClean, Cornelius Hempel, Peter J Love, and Alán Aspuru-Guzik, "Strategies for quantum computing molecular energies using the unitary coupled cluster ansatz," Quantum Sci. Technol. **4**, 014008 (2019).
[30] Harper R. Grimsley, Sophia E. Economou, Edwin Barnes, and Nicholas J. Mayhall, "An adaptive variational algorithm for exact molecular simulations on a quantum computer," Nat Commun **10**, 3007 (2019).
[31] S. Cohen and D. Kurath, "Effective interactions for the 1p shell," Nuclear Physics **73**, 1–24 (1965).
[32] P. Jordan and E. Wigner, "Über das paulische Äquivalenzverbot," Z. Physik **47**, 631–651 (1928).
[33] Sergey B. Bravyi and Alexei Yu. Kitaev, "Fermionic quantum computation," Annals of Physics **298**, 210–226 (2002).
[34] Andrew Tranter, Peter J. Love, Florian Mintert, and Peter V. Coveney, "A comparison of the bravyi–kitaev and jordan–wigner transformations for the quantum simulation of quantum chemistry," Journal of Chemical Theory and Computation **14**, 5617–5630 (2018), pMID: 30189144, https://doi.org/10.1021/acs.jctc.8b00450.
[35] Dean Lee, "Lattice simulations for few- and many-body systems," Prog. Part. Nucl. Phys. **63**, 117 – 154 (2009).
[36] Pranav Gokhale, Olivia Angiuli, Yongshan Ding, Kaiwen Gui, Teague Tomesh, Martin Suchara, Margaret Martonosi, and Frederic T. Chong, "Optimization of simultaneous measurement for variational quantum eigensolver applications," in *2020 IEEE International Conference on Quantum Computing and Engineering (QCE)* (2020) pp. 379–390.

[37] Daniel Miller, Laurin E. Fischer, Igor O. Sokolov, Panagiotis Kl. Barkoutsos, and Ivano Tavernelli, "Hardware-tailored diagonalization circuits," ArXiv e-prints (2022), arXiv:2203.03646v1 [quant-ph].

[38] William J. Huggins, Jarrod R. McClean, Nicholas C. Rubin, Zhang Jiang, Nathan Wiebe, K. Birgitta Whaley, and Ryan Babbush, "Efficient and noise resilient measurements for quantum chemistry on near-term quantum computers," npj Quantum Inf **7**, 23 (2021).

[39] Guillermo García-Pérez, Matteo A.C. Rossi, Boris Sokolov, Francesco Tacchino, Panagiotis Kl. Barkoutsos, Guglielmo Mazzola, Ivano Tavernelli, and Sabrina Maniscalco, "Learning to measure: Adaptive informationally complete generalized measurements for quantum algorithms," PRX Quantum **2**, 040342 (2021).

[40] Francesco A. Evangelista, Garnet Kin-Lic Chan, and Gustavo E. Scuseria, "Exact parameterization of fermionic wave functions via unitary coupled cluster theory," The Journal of Chemical Physics **151**, 244112 (2019).

[41] Oscar Higgott, Daochen Wang, and Stephen Brierley, "Variational quantum computation of excited states," Quantum **3**, 156 (2019).

[42] Jules Tilly, Glenn Jones, Hongxiang Chen, Leonard Wossnig, and Edward Grant, "Computation of molecular excited states on ibm quantum computers using a discriminative variational quantum eigensolver," Phys. Rev. A **102**, 062425 (2020).

[43] Pauline J. Ollitrault, Abhinav Kandala, Chun-Fu Chen, Panagiotis Kl. Barkoutsos, Antonio Mezzacapo, Marco Pistoia, Sarah Sheldon, Stefan Woerner, Jay M. Gambetta, and Ivano Tavernelli, "Quantum equation of motion for computing molecular excitation energies on a noisy quantum processor," Phys. Rev. Research **2**, 043140 (2020).

[44] Earl Campbell, "Random compiler for fast hamiltonian simulation," Phys. Rev. Lett. **123**, 070503 (2019).

[45] Andrea Skolik, Jarrod R. McClean, Masoud Mohseni, Patrick van der Smagt, and Martin Leib, "Layerwise learning for quantum neural networks," Quantum machine intelligence **3**, 5 (2021).

[46] Yordan S. Yordanov, David R. M. Arvidsson-Shukur, and Crispin H. W. Barnes, "Efficient quantum circuits for quantum computational chemistry," Phys. Rev. A **102**, 062612 (2020).

[47] Yordan S. Yordanov, V. Armaos, Crispin H. W. Barnes, and David R. M. Arvidsson-Shukur, "Qubit-excitation-based adaptive variational quantum eigensolver," Nat Commun **4**, 228 (2021).

[48] M. Cerezo, Akira Sone, Tyler Volkoff, Lukasz Cincio, and Patrick J. Coles, "Cost function dependent barren plateaus in shallow parametrized quantum circuits," Nature Communications **12**, 1791 (2021).

[49] J.C. Spall, "Implementation of the simultaneous perturbation algorithm for stochastic optimization," IEEE Transactions on Aerospace and Electronic Systems **34**, 817–823 (1998).

[50] Edward Grant, Leonard Wossnig, Mateusz Ostaszewski, and Marcello Benedetti, "An initialization strategy for addressing barren plateaus in parametrized quantum circuits," Quantum **3**, 214 (2019).

[51] Julien Gacon, Christa Zoufal, Giuseppe Carleo, and Stefan Woerner, "Simultaneous perturbation stochastic approximation of the quantum fisher information," Quantum **5**, 567 (2021).

[52] MD SAJID ANIS *et al.*, "Qiskit: An open-source framework for quantum computing," (2021).

[53] Ville Bergholm, Josh Izaac, Maria Schuld, Christian Gogolin, Shahnawaz Ahmed M. Sohaib Alam, Juan Miguel Arrazola, Carsten Blank, Alain Delgado, Soran Jahangiri, Keri McKiernan, Johannes Jakob Meyer, Zeyue Niu, Antal Száva, and Nathan Killoran, "Pennylane: Automatic differentiation of hybrid quantum-classical computations," ArXiv e-prints (2018), arXiv:1811.04968 [quant-ph].

[54] Gushu Li, Yufei Ding, and Yuan Xie, "Tackling the qubit mapping problem for nisq-era quantum devices," in *Proceedings of the Twenty-Fourth International Conference on Architectural Support for Programming Languages and Operating Systems*, ASPLOS '19 (Association for Computing Machinery, New York, NY, USA, 2019) p. 1001–1014.

[55] Paul D. Nation, Hwajung Kang, Neereja Sundaresan, and Jay M. Gambetta, "Scalable mitigation of measurement errors on quantum computers," PRX Quantum **2**, 040326 (2021).

[56] Andre He, Benjamin Nachman, Wibe A. de Jong, and Christian W. Bauer, "Zero-noise extrapolation for quantum-gate error mitigation with identity insertions," Phys. Rev. A **102**, 012426 (2020).

[57] Kristan Temme, Sergey Bravyi, and Jay M. Gambetta, "Error mitigation for short-depth quantum circuits," Phys. Rev. Lett. **119**, 180509 (2017).

[58] Abhinav Kandala, Kristan Temme, Antonio D. Córcoles, Antonio Mezzacapo, Jerry M. Chow, and Jay M. Gambetta, "Error mitigation extends the computational reach of a noisy quantum processor," Nature **567**, 491–495 (2019).